NEOPLASIA
www.neoplasia.com

Volume 19 Number 3 March 2017 pp. 216–225 216

Loss of *Pin1* Suppresses Hedgehog-Driven Medulloblastoma Tumorigenesis[1]

Tao Xu[*,2], Honglai Zhang[*,2], Sung-Soo Park[*,2], Sriram Venneti[*], Rork Kuick[†], Kimberly Ha[*], Lowell Evan Michael[‡], Mariarita Santi[§], Chiyoko Uchida[¶], Takafumi Uchida[#], Ashok Srinivasan[**], James M. Olson[††], Andrzej A. Dlugosz[‡], Sandra Camelo-Piragua[*] and Jean-François Rual[*]

[*]Department of Pathology, University of Michigan Medical School, Ann Arbor, MI 48109, USA; [†]Center for Cancer Biostatistics, School of Public Health, University of Michigan, Ann Arbor, MI 48109, USA; [‡]Departments of Dermatology and Cell & Developmental Biology, University of Michigan School of Medicine, Ann Arbor, MI 48109, USA; [§]Department of Pathology, Children's Hospital of Philadelphia, Philadelphia, PA 19104, USA; [¶]Department of Human Development and Culture, Fukushima University, Fukushima, 960-1296, Japan; [#]Department of Molecular Cell Science, Tohoku University, Sendai 981-8555, Japan; [**]Department of Radiology, University of Michigan Medical School, Ann Arbor, MI 48109, USA; [††]Fred Hutchinson Cancer Research Center, Seattle, WA 98109, USA

Abstract

Medulloblastoma is the most common malignant brain tumor in children. Therapeutic approaches to medulloblastoma (combination of surgery, radiotherapy, and chemotherapy) have led to significant improvements, but these are achieved at a high cost to quality of life. Alternative therapeutic approaches are needed. Genetic mutations leading to the activation of the Hedgehog pathway drive tumorigenesis in ~30% of medulloblastoma. In a yeast two-hybrid proteomic screen, we discovered a novel interaction between GLI1, a key transcription factor for the mediation of Hedgehog signals, and PIN1, a peptidylprolyl cis/trans isomerase that regulates the postphosphorylation fate of its targets. The GLI1/PIN1 interaction was validated by reciprocal pulldowns using epitope-tagged proteins in HEK293T cells as well as by co-immunoprecipiations of the endogenous proteins in a medulloblastoma cell line. Our results support a molecular model in which PIN1 promotes GLI1 protein abundance, thus contributing to the positive regulation of Hedgehog signals. Most importantly, *in vivo* functional analyses of *Pin1* in the *GFAP-tTA;TRE-SmoA1* mouse model of Hedgehog-driven medulloblastoma demonstrate that the loss of *Pin1* impairs tumor development and dramatically increases survival. In summary, the discovery of the GLI1/PIN1 interaction uncovers PIN1 as a novel therapeutic target in Hedgehog-driven medulloblastoma tumorigenesis.

Neoplasia (2017) 19, 216–225

Abbreviations: AD, activation domain; CGNP, cerebellar granular neuron progenitor cells; CIP, calf intestinal alkaline phosphatase; DB, DNA-binding domain; EGCG, epigallocatechin gallate; FFPE, formalin-fixed, paraffin-embedded; H&E, hematoxylin/eosin staining; Hh, Hedgehog; IHC, immunohistochemistry; IP, immunoprecipitation; MRI, magnetic resonance imaging; PPIase, peptidylprolyl cis/trans isomerase; pSer/Thr-Pro, phosphorylated serine-proline or threonine-proline motifs; tTA, tetracycline-regulated transactivators; TRE, tetracycline responsive element; SAG, SMO agonist; SBP, streptavidin binding peptide tag; WB, Western blot; Y2H, yeast two-hybrid

Address all correspondence to: Sandra Camelo-Piragua or Jean-François Rual, Department of Pathology, University of Michigan Medical School, Ann Arbor, MI 48109, USA.
E-mail: sandraca@umich.edu, jrual@umich.edu

[1] Conflicts of Interest: The authors declare no conflict of interest.

[2] These authors contributed equally to this work.

Received 30 December 2016; Accepted 9 January 2017

1476-5586
http://dx.doi.org/10.1016/j.neo.2017.01.002

Introduction

Medulloblastoma is the most common malignant brain tumor of childhood [1]. Genomics applied to medulloblastoma identified four medulloblastoma subgroups, each characterized by a distinct molecular and clinical profile (Wnt, Hh, groups 3 and 4) [1,2]. Current therapeutic approaches to medulloblastoma are based on surgery, radiation, and nontargeted chemotherapy, and are indistinguishably applied to all medulloblastoma subgroups. These therapies have led to significant improvements, with a 70% 5-year survival rate, but these results are achieved at a high cost to quality of life, e.g., cognitive or hormonal deficiencies, resulting from the effects of nonspecific, antimitotic agents on the developing brains of young medulloblastoma patients [3,4]. Alternative therapeutic approaches are needed, and molecular stratification of medulloblastoma patients has yet to be routinely implemented in the clinic.

Hedgehog (Hh) signaling is an essential contributor to tumorigenesis for ~30% of medulloblastoma patients [1,2]. At the molecular level, canonical Hh signaling involves the binding of a secreted Hh ligand, e.g., Sonic Hedgehog, to a membrane-bound Patched receptor, e.g., PTCH1. In the absence of ligand binding, PTCH1 inhibits SMO, a membrane-bound G-protein–coupled receptor-like molecule and a positive regulator of Hh signals. In the absence of activated SMO, GLI transcription factors are sequestered in the cytoplasm in a complex containing the negative regulator SUFU (applicable to GLI1, 2 and 3) and/or present as processed repressor forms (applicable to GLI2 and 3, not GLI1). Upon ligand binding, inhibition of PTCH1 leads to the de-repression of SMO. Activated SMO orchestrates a signaling cascade that eventually results in the release and translocation of activated GLI transcription factors into the nucleus. GLI transcription factors positively regulate the expression of various context-specific Hh-signal effectors that govern cell fate, e.g., *CCND1* and *MYCN,* as well as *PTCH1* itself, thus forming a negative feedback loop [5,6]. Genetic alterations observed in Hh-medulloblastoma patients include loss of function mutations in the genes of negative regulators of Hh, e.g., *PTCH1* and *SUFU,* as well as gain-of-function mutations of *SMO* and gene amplifications of other positive regulators or downstream targets of Hh, e.g., *GLI2* and *MYCN*[7].

Our objective is to discover Hh pathway protein interactors and signal modulators that are essential for maintaining oncogenic Hh signaling and tumorigenesis in medulloblastoma. Using a proteomic platform for systematic protein interaction mapping, we discovered a novel interaction between GLI1 and PIN1, a conserved enzyme that catalyzes the cis/trans isomerization of peptidyl-prolyl peptide bonds [8–11]. The peptidylprolyl cis/trans isomerase (PPIase) activity of PIN1 is specifically aimed at phosphorylated Serine-Proline or Threonine-Proline motifs (pSer/Thr-Pro), thereby regulating the postphosphorylation conformation of its substrates in various physiological and pathophysiological conditions [8–12]. Although *Pin1* KO mice display a range of cell-proliferative abnormalities, e.g., decreased body weight [13], they develop essentially normally [14]. PIN1 may be implicated in the amplification of oncogenic signals, as shown by its frequent overexpression in several human malignancies [15–17], including brain tumors [18]. However, there are no reports to date linking PIN1 to medulloblastoma tumorigenesis.

In light of the novel GLI1/PIN1 interaction and the previous reports that PIN1 interacts with other key positive regulators of Hh-medulloblastoma, e.g., CCND1 [13], NANOG [19], NOTCH1 [20] and PLK1 [21], we hypothesized that PIN1 promotes Hh-medulloblastoma tumorigenesis. In the present study, we investigated the loss of *Pin1* in a mouse model of Hh-medulloblastoma. Our results demonstrate that loss of *Pin1* suppresses tumorigenesis, thus identifying a novel therapeutic target in this disease context.

Materials and Methods

Reagents

The protein-encoding ORFs of GLI1 and PIN1 cloned as Gateway Entry (Thermo Fisher Scientific, Waltham, MA) clones were obtained from the Center for Cancer Systems Biology (CCSB, Dana-Farber Cancer Institute, Boston, MA) human ORFeome v8.1 collection or cloned by Gateway recombination cloning from cDNA plasmids as previously described [22]. The PIN1 mutant PIN1 ^{W34A} was generated by site-directed mutagenesis from WT PIN1 Entry clone. The pcDNA3-HA-DEST and pDEST-GEX5X protein expression vectors were kindly provided by Dr. Siming Li (University of Michigan). The pBABE-SFB (S-FLAG-SBP triple tags) vector was provided by Dr. Jun. Huang (Zhejiang University, China). The yeast two-hybrid (Y2H) pDEST-DB and pDEST-AD vectors were generously provided by the CCSB. The Sonic hedgehog N-Terminus (Shh-N) plasmid was provided by Dr. Benjamin Allen (University of Michigan). The sh-*PIN1* construct was obtained from Open Biosystems (Oligo ID#: V2LHS58415). The following primary antibodies were used: PIN1 (Santa Cruz Biotechnology, Santa Cruz, CA, sc15340 and sc46660), GLI1 (Cell Signaling, Danvers, MA, #2534, #2643; Novus, Littleton, CO, NB600-600), NeuN (Zymed, Thermo Fisher Scientific, Waltham, MA, #18-7373), Ki67 (Abcam, Cambridge, MA, ab16667), HA (Roche, Reinach, Switzerland, #12013819001), FLAG (Sigma, St. Louis, MO, A8592), and β-actin (Cell Signaling, #5125). Secondary antibodies were purchased from Cell Signaling (goat α-rabbit IgG, #7074 and horse α-mouse IgG, #7076). *Juglone* was purchased from Sigma (H47003). *SAG* was purchased from EMD Millipore, Billerica, MA (Cat: 566660). CRISPR/Cas9 guide sequences targeting the *GLI1* and *PIN1* genes were designed as previously described [23] and cloned into the lentiCRISPR CRISPR/Cas9 plasmid (Addgene, Cambridge, MA, 49535) using a previously described method [24].

Cell Lines and Cell Culture Conditions

MED-311FH is a low-passage, patient-derived cell line derived from a medulloblastoma tumor, which was recently generated by the Fred Hutchinson Cancer Research Center (FHCRC) Brain Tumor Resource Laboratory. MED-311FH was obtained by the Rual lab from FHCRC on 10/2015. Cell line authentication was performed by STR profiling. We note that MED-311FH had originally been classified as Hh-medulloblastoma by nanoString [25]; however, it was recently reclassified as an atypical medulloblastoma in genomewide 450k methylation analyses. Molecular studies were also performed in the following cell lines: 22Rv1 (human prostate carcinoma) and HEK293T (human embryonic kidney). 22Rv1 and HEK293T were obtained from ATCC, Manassas, VA prior to 2013. Cells were maintained in cell culture by following provider's instructions. Protein expression vectors were transfected into the cells using polyethylenimine, as described previously [26], or by lentiviral/retroviral transduction, using standard protocols. After transduction with the *sh-PIN1* or *sh-Scramble* short hairpin RNA interference constructs, puromycin (2 μg/ml; Sigma, P8833) was included to ensure selection for presence of the plasmids. All cell lines have been tested for mycoplasma contamination.

Y2H

Y2H screens were performed as described previously [27].

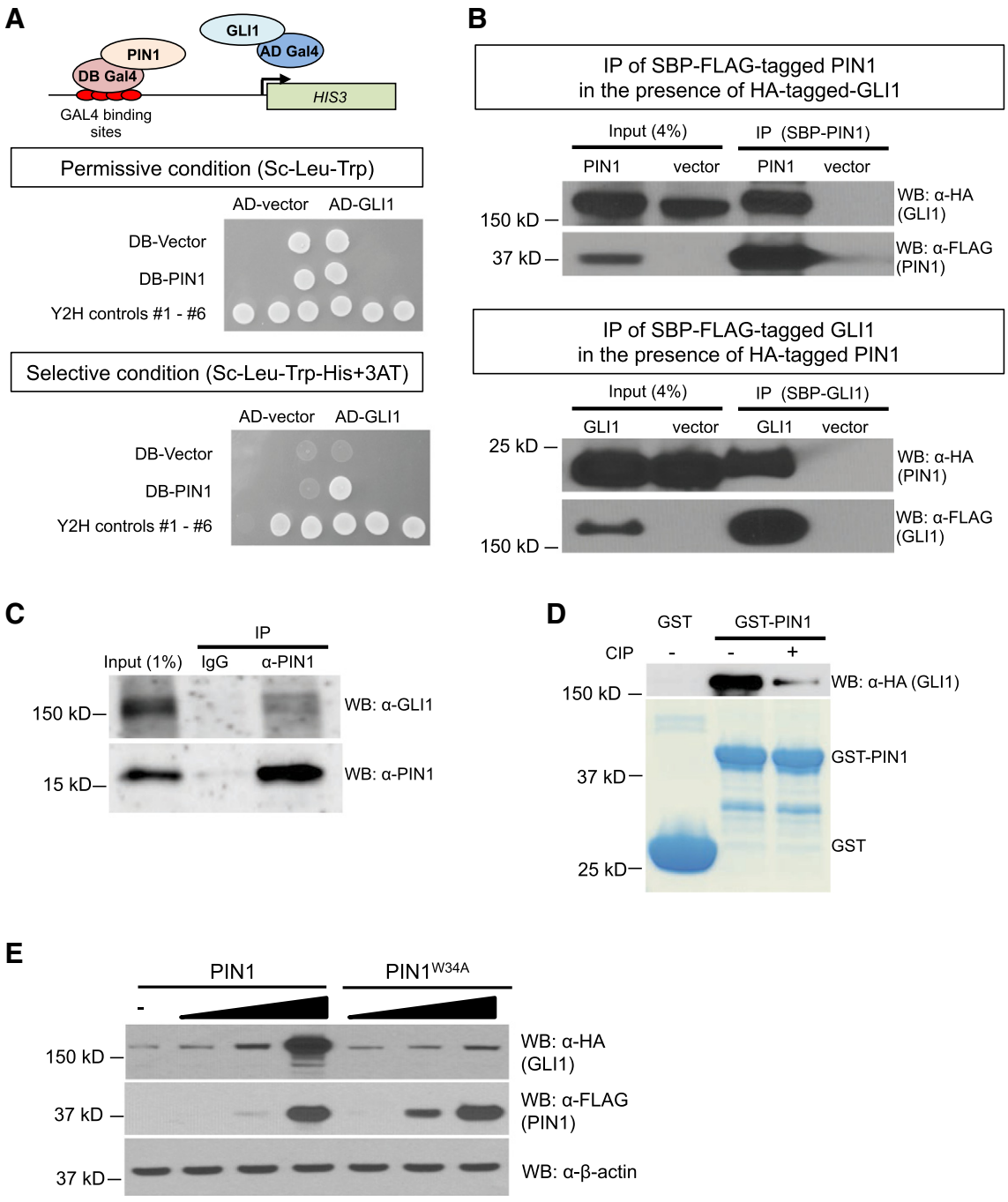

Figure 1. GLI1 interacts with PIN1. (A) Detection of the GLI1/PIN1 interaction using the Y2H assay. In this Y2H experiment, PIN1 is fused to the GAL4 DNA-binding (DB) domain and GLI1 is fused to the GAL4 activation domain (AD). The six Y2H controls have been previously described [27]. The DB-PIN1 and AD-GLI1 fusion proteins interact with each other, leading to the activation of the *HIS3* reporter gene and allowing yeast cells to grow on selective medium lacking histidine. Experiment was replicated three times. (B) HA-GLI1 co-purifies with SBP-FLAG-PIN1 (top panels), and HA-PIN1 co-purifies with SBP-FLAG-GLI1 (bottom panels). Immunoprecipitation (IP) of SBP-FLAG–tagged PIN1 (top panels) or SBP-FLAG–tagged GLI1 (bottom panels) in HEK293T cells in the presence of HA-tagged GLI1 or HA-tagged PIN1, respectively. WB: Western blot; SBP: Streptavidin binding peptide tag. Experiment was replicated three times. (C) Endogenous GLI1 co-purifies with endogenous PIN1 in MED-311FH cells, a low-passage, patient-derived cell line derived from a medulloblastoma tumor. The IP of endogenous PIN1 was performed using an α-PIN1 monoclonal antibody on a protein extract derived from Shh-N ligand-treated MED-311FH cells, followed by Western blot analyses using either α-PIN1 or α-GLI1 antibody. Experiment was replicated twice. WB: Western blot; IP: immunoprecipitation. (D) PIN1 interacts with GLI1 in a phosphorylation-dependent manner. GST pulldown with glutathione beads of bacteria-purified GST-tagged PIN1 in the presence of a protein extract derived from mammalian HEK293T cells transduced with HA-tagged GLI1 and in the presence or absence of calf intestinal alkaline phosphatase (CIP). Experiment was replicated twice. WB: Western blot. (E) PIN1 leads to increased GLI1 protein abundance *in vitro*. Analysis of GLI1 protein levels in the presence of an increasing level of WT PIN1 and mutant PIN1^{W34A} in HEK293T cells. HEK293T cells were transfected with 300 ng of HA-GLI1 protein expression vector as well as 0, 50, 150, or 450 ng of the SBP-FLAG-PIN1 or the SBP-FLAG-PIN1^{W34A} protein expression vector. Experiment was replicated twice. WB: Western blot; SBP: Streptavidin binding peptide tag.

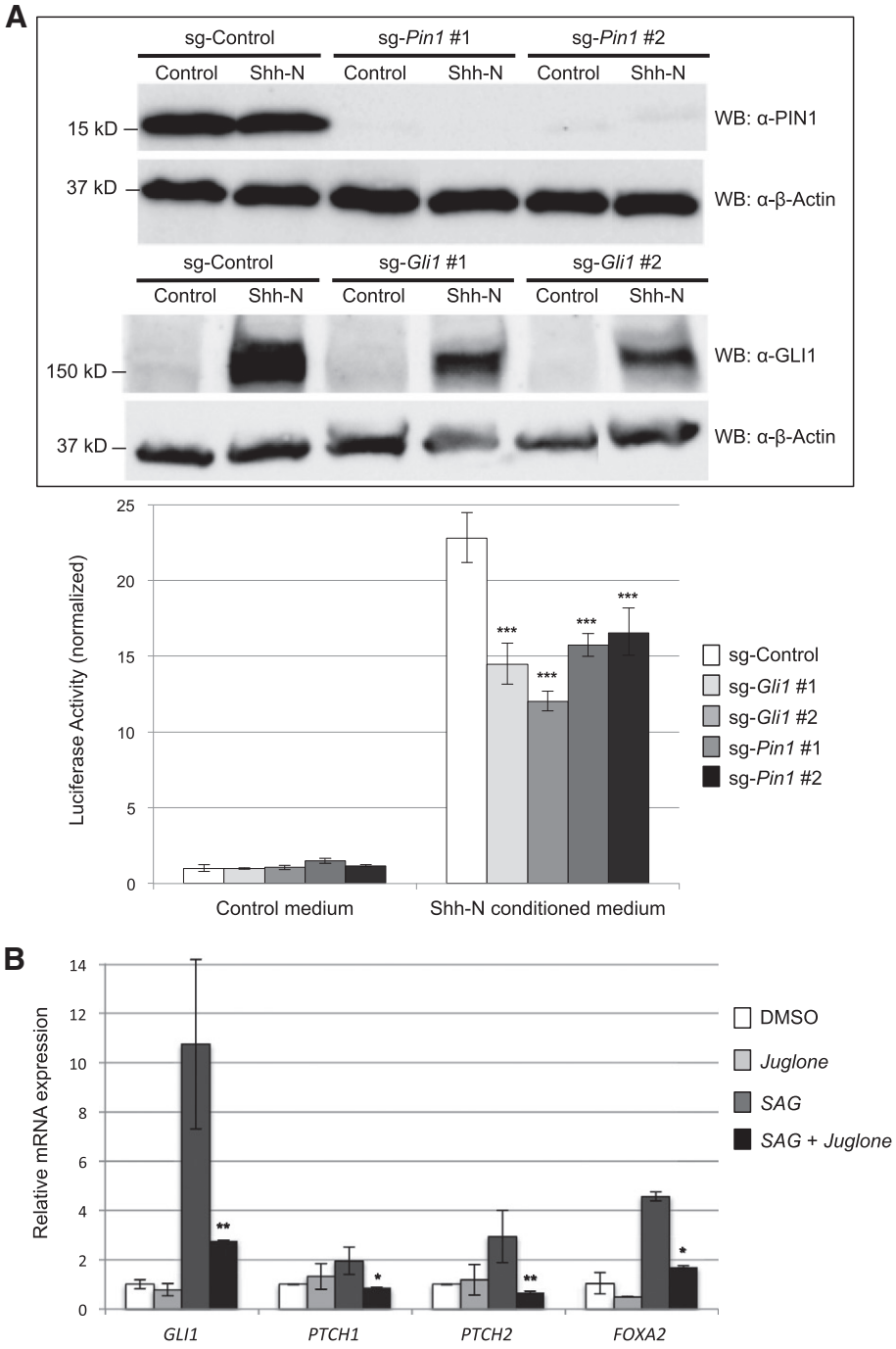

Figure 2. PIN1 promotes Hh signaling. (A) GLI-dependent luciferase reporter assay. Shh-Light2 is an NIH 3T3 cell line stably transfected with GLI-dependent Firefly luciferase and constitutive Renilla luciferase reporters, which can be used to study modulation of Hh signaling [35]. Shh-N–mediated activation of luciferase activities was measured upon CRISPR/Cas9-mediated depletion of either GLI1 or PIN1. Control: Shh-Light2 cells stably transfected with empty CRISPR/Cas9 vector. First, for each one of the 10 conditions tested, the Firefly luciferase activity signals were measured using the Dual-Luciferase Reporter Assay System (Promega) and were normalized by the Renilla luciferase signals. Second, the 10 signal ratios were normalized by the signal ratio obtained in the [control medium/control cell line] condition. Shown are means ±S.D. of three biological replicates. We fit analysis of variance (ANOVA) models to log-transformed data and tested whether the increase with Shh-N versus no treatment was smaller under *Gli1* and *Pin1* KD conditions than the same increase under control conditions. The difference of fold-changes was significant for all four KD conditions tested; [***] $P < 3 \times 10^{-5}$. Inset: Western blot analyses validate the CRISPR/Cas9-mediated depletion of PIN1 and GLI1. sg: CRISPR/Cas9 single guide RNA; WB: Western blot. (B) Expression analysis by quantitative RT-PCR of Hh target genes upon treatment with *SAG* (0.3 μM) and/or *juglone* (5 μM) in MED-311FH. Shown are means ± S.D. of two biological replicates measured twice each. Statistical significances of the difference between the "*SAG*" and "*SAG* + juglone" conditions were computed using one-way ANOVA models on log-transformed data for each gene; [*] $P < .05$, [**] $P < .01$.

Co-Immunoprecipitation of the Endogenous PIN1 and GLI1 Proteins

MED-311FH and 22Rv1 cells were grown in Shh-N conditioned medium for 48 hours. Cells were treated with 10 μM MG132 (Sigma, C2211) for 12 hours to block the 26S proteasome. For immunoprecipitation, cells were harvested and lysed with lysis buffer (50 mM Tris pH 8.0, 150 mM NaCl, 0.5% NP-40, 2 mM EDTA, Complete protease inhibitor (Roche, Reinach, Switzerland). The supernatant fraction was recovered and immunoprecipitated with α-PIN1antibody (Epitomics, Abcam, Cambridge, MA, 2136–1, 1:50 or Santa Cruz Biotechnology, Santa Cruz, CA, sc15340, 1:30) and 30 μl Protein A/G-Sepharose (Sigma, P9424/P3296, 1:1). After three washes with lysis buffer, purified protein extracts were resuspended in 2× LDS sample

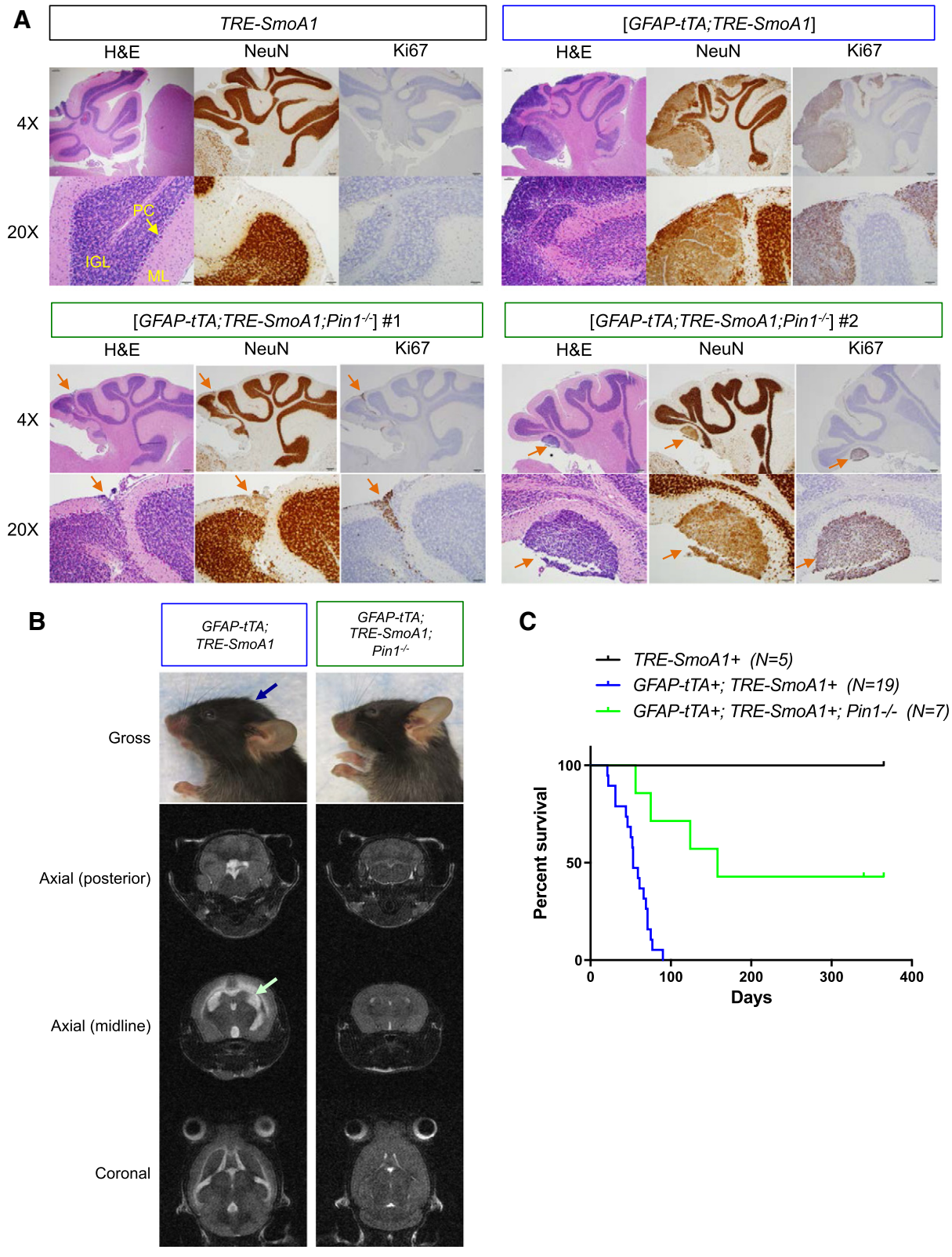

buffer, separated on acrylamide gels, transferred to PVDF membranes, and immunoblot-analyzed with either α-GLI1 antibody (Cell Signaling, #2643) or α-PIN1 antibody (Santa Cruz Biotechnology, sc46660).

SBP-Tag Protein Pulldowns in HEK293T Cells

HEK293T cells transfected with protein expression vector or "empty" negative control vector were cultured in Dulbecco's modified Eagle's medium supplemented with 10% fetal bovine serum. Cells were harvested and lysed on ice for 30 minutes in a lysis buffer [50 mM Tris pH 8.0, 150 mM NaCl, 0.5% NP-40, 2 mM EDTA, Complete protease inhibitor (Roche, 05056489001)]. Cell lysates were cleared by centrifugation for 10 minutes at 16,000×*g*, and protein complexes were incubated with 30 μl of streptavidin agarose resin (Thermo Fisher Scientific, Waltham, MA, 20361) for 4 hours at 4°C. The beads were washed three times with 1 ml of lysis buffer. Then proteins were eluted by boiling for 5 minutes in 2× LDS sample buffer (Invitrogen, Thermo Fisher Scientific, Waltham, MA, NP0008). Purified protein extracts and input control lysate samples were then separated on acrylamide gels and transferred to PVDF membranes, and proteins were detected using standard immunoblotting techniques using the antibodies described above.

GST Pulldowns

For purification of recombinant PIN1 protein, WT or mutant PIN1 protein-encoding ORFs were Gateway-cloned into pDEST-GEX5X (an N-terminal GST-tagged protein, bacterial expression vector) and transformed into *Escherichia coli* BL21(DE3). Expression of the recombinant proteins was induced with 0.3 mM IPTG at 16°C. After overnight culture, cells were collected by centrifugation, resuspended in lysis buffer (50 mM Tris pH 7.5, 150 mM NaCl, 0.05% NP-40, 1 mM PMSF, and Complete protease inhibitor), and sonicated. After centrifugation, the cleared supernatants were collected and incubated with 50 μl of washed glutathione sepharose (GE Healthcare, Livonia, MI, 17-0756-01) for 4 hours at 4°C. The "GST-alone" or the GST-PIN1 protein-bound glutathione beads were then washed three times with 1 ml of lysis buffer. For the GST pulldown assay, HA-GLI1 was transient transfected into HEK293T cells. Cells were harvested 48 hours after transfection and lysed with lysis buffer. The cleared cell lysates were incubated with the "GST-alone" or the GST-PIN1 protein-bound glutathione beads for 2 hours at 4°C. The beads were washed five times with lysis buffer and subjected to immunoblotting analysis.

Confocal Microscopic Analysis

HEK293T cells were transfected with plasmids expressing GFP-GLI1 and RFP-PIN1 for 24 hours in a glass-bottom culture dish coated with Poly-d-lysine (MatTek, Ashland, MA, P35GC-1.5-14-C). Fluorescence images were obtained using a Nikon A1 (Melville, NY) confocal microscope.

Luciferase Reporter Assay

Shh-Light2 cells (GRCF Biorepository & Cell Center, Johns Hopkins School of Medicine) were treated with Shh-N conditioned medium for 48 hours. Dual-luciferase reporter assays were performed using the Dual-Luciferase Reporter Assay System (Promega, Madison, WI) according to the manufacturer's instructions, and data were collected on a SpectraMax M5 plate reader (Molecular Devices, Sunnyvale, CA).

Gene Expression Analysis

Total RNA was extracted with Trizol reagent (Ambion, Thermo Fisher Scientific, Waltham, MA, 15596018) using manufacturer's instructions and further purified with the RNeasy Mini Kit (Qiagen, Hilden, Germany, 74106). Five micrograms of RNA was reverse-transcribed in cDNA using oligo(dT)18-primed reverse transcription and SuperScript III RT First-Strand kit (Invitrogen, 18080-051) as described by the manufacturer. The cDNA was analyzed via quantitative polymerase chain reaction (qPCR) analysis using the Power SYBR Green PCR master mix (Applied Biosystems, Thermo Fisher Scientific, Waltham, MA, 4367662) and the CFX96 Touch Real-Time PCR Detection System (BioRad, Hercules, CA) according to manufacturer's recommendations. Data were normalized to the housekeeping gene glyceraldehyde 3-phosphate dehydrogenase (GAPDH). Primers used in RT-qPCR experiments are listed in Supplementary Table 1.

[GFAP-tTA;TRE-SmoA1] Mouse Model

We studied medulloblastoma tumorigenesis in the absence or presence of *Pin1* in the previously published bitransgenic [*GFAP-tTA;TRE-SmoA1*] model [28], where the expression of the tetracycline-regulated transactivators (*tTA*) is driven by a GFAP promoter and the expression of oncogenic *SmoA1* is under the control of the tetracycline responsive element (*TRE*). The experimental breeders used in this study were a *Pin1* KO mouse [14], a *TRE-SmoA1* mouse [28], and a *GFAP-tTA* mouse [29], all of which were maintained on a C57/BL6 background for at least five generations prior to initiating experiments. *TRE-SmoA1*, [*GFAP-tTA;TRE-SmoA1*], and [*GFAP-tTA;TRE-SmoA1;Pin1*$^{-/-}$] mouse littermates were generated by crossing [*GFAP-tTA;Pin1*$^{-/+}$] mice with [*TRE-SmoA1;Pin1*$^{-/+}$] mice. Maintenance of mouse colonies and experimental procedures were approved by the University of Michigan University Committee on the Use and Care of Animals.

Figure 3. Loss of *Pin1* impairs Hh-medulloblastoma tumorigenesis *in vivo*. (A) Histopathological examination of the cerebellums of one P21 *TRE-SmoA1* mouse, one P21 [*GFAP-tTA;TRE-SmoA1*] mouse, and two P21 [*GFAP-tTA;TRE-SmoA1;Pin1*$^{-/-}$] mice by H&E staining as well as by Ki67 (marker of proliferation) and NeuN (marker of neuronal differentiation) IHC on 5-μm–thick FFPE tissue sections (magnification: 4× and 20×). The different cell layers of the cerebellum, i.e., the molecular (ML), Purkinje cell (PC), and internal granular cell (IGL) layers, are labeled in the 20× *TRE-SmoA1* control H&E picture. Note: the 20× pictures of the [*GFAP-tTA;TRE-SmoA1;Pin1*$^{-/-}$] mice focus on the microscopic tumors (orange arrows), which are detected in <5% of the cerebellums, and thus are not representative of the whole [*GFAP-tTA;TRE-SmoA1;Pin1*$^{-/-}$] cerebellums which, for the most part, appear normal. (B) MRI analysis of the cerebellums of P56 [*GFAP-tTA;TRE-SmoA1;Pin1*$^{-/-}$] and [*GFAP-tTA;TRE-SMOA1*] littermates. For the [*GFAP-tTA;TRE-SmoA1*] mouse, 1) doming of the skull can be grossly appreciated (blue arrow); 2) the axial (posterior) MRI film shows an enlarged [*GFAP-tTA;TRE-SmoA1*] cerebellum; and 3) the axial (midline) and coronal films demonstrate dilatation of the ventricles and subarachnoid spaces (green arrow). In contrast, analysis of the [*GFAP-tTA;TRE-SmoA1;Pin1*$^{-/-}$] mouse does not reveal any such signs of tumor burden. (c) Kaplan-Meier analysis of *Pin1* in *SmoA1*-driven medulloblastoma. Three groups of *C57BL/6* mice were assessed for survival: 1) *TRE-SmoA1*, 2) [*GFAP-tTA;TRE-SmoA1*], and 3) [*GFAP-tTA;TRE-SmoA1;Pin1*$^{-/-}$]. [*GFAP-tTA;TRE-SmoA1;Pin1*$^{-/-}$] mice survived significantly longer than [*GFAP-tTA;TRE-SmoA1*] mice [$P = .0005$, log rank test]. No randomization was used, and no blinding was done.

Mouse Genotyping

Pups were genotyped between P14 and P21 by PCR analysis. The presence of the GFAP-tTA transgene was ascertained by individual PCR for the tetracycline transactivator (5′-ctcgcccagaagctaggtgt-3′ and 5′-ccatcgcgatgacttagt-3′). A *TRE-SmoA1* genotype was assessed by PCR amplification of the SV40 poly-A tail (5′-ggaactgatgaatgggagca-3′ and 5′-gggaggtgtgggaggttt-3′). The *Pin1* WT versus KO genotype was ascertained by PCR targeting the *Pin1* gene locus (forward: 5′-gcacccgatcctgttctgcaaactcag-3′, WT reverse: 5′-catgagaagggattagaag caagattcgactgg-3′, or mutant reverse: 5′-gccagaggccacttgtgtagcgc-3′).

Magnetic Resonance Imaging (MRI)

Medulloblastoma tumor growth was monitored *in vivo,* noninvasively, by MRI analysis at the University of Michigan Center for Molecular Imaging. Isoflurane-anesthetized animals were laid prone, head first in a 7.0-T Agilent (Santa Clara, CA) MR scanner with the body temperature maintained at 37°C using forced heated air. A quadrature volume radiofrequency coil was used to scan the head region of the mice. Axial and coronal T2-weighted images were acquired using a fast spin-echo sequence with the following parameters: repetition time/effective echo time, 4000/60 milliseconds; number of echoes, 8; field of view, 20 × 20 mm; matrix, 256 × 128; slice thickness, 0.5 mm; number of slices, 25.

Immunohistochemistry

Immunohistochemistry (IHC) was performed on 5-μm–thick formalin-fixed, paraffin-embedded (FFPE) tissue sections. Antigen retrieval was performed with Reveal Decloaker (Biocare Medical, Concord, CA, RV1000; for Ki67 IHC) or by heat-induced epitope retrieval in 10 mM sodium citrate pH 6 buffer (for NeuN IHC). IHC was performed using the DAKO Autostainer (Troy, MI). Sections were stained with the following primary antibodies for 1 hour at ambient temperature: a rabbit polyclonal antibody to Ki67 (Abcam, ab16667, 1:500-diluted) and a purified mouse monoclonal antibody to NeuN (EMD Millipore, Billerica, MA, MAB377, 1:200-diluted). After primary antibody incubation and washing, a polymer horseradish peroxidase secondary antibody [Biocare Medical, RMR622 (for Ki67 IHC) or Envision+, Agilent, Santa Clara, CA, K4000 (for NeuN IHC)] was applied. Chromogen diaminobenzidine was applied for visualization and slides counterstained with hematoxylin.

Results

GLI1 Interacts with PIN1

GLI1 is a key factor in the Hh pathway that contributes to the amplification of Hh signals. In mouse, *Gli1* is not required for development or viability [30,31]. However, loss of *Gli1* impairs Hh-medulloblastoma tumorigenesis [32–34]. Using a proteomic approach, we obtained multiple, independent lines of evidence supporting a molecular interaction between GLI1 and PIN1. First, we discovered the GLI1/PIN1 interaction in a Y2H screen (Figure 1*A*). Second, the GLI1/PIN1 interaction was validated by reciprocal pulldowns using epitope-tagged proteins in HEK293T cells (Figure 1*B*). Third, we performed immunoprecipitations of endogenous PIN1 in MED-311FH cells, a low-passage cell line derived from a medulloblastoma patient, and in 22Rv1, a human prostate carcinoma cell line. In both immunoprecipitates, we observed that endogenous GLI1 co-purifies with endogenous PIN1 (Figure 1*C* and Supplementary Figure 1). Fourth, in a confocal microscopy analysis, we observed that GFP-GLI1 co-localizes with RFP-PIN1 in the nucleus of HEK293T cells (Supplementary Figure 2). Fifth, we observed that the WW domain of PIN1 is required for the interaction, as verified by the analysis of the PIN1^{W34A} point mutant, which fails to co-purify with GLI1 (Supplementary Figure 3).

PIN1 binds pSer/Thr-Pro motifs [8–11]. Thus, a phosphorylation event likely precedes the binding of PIN1 to its target. Upon investigating the phosphorylation dependence of the GLI1/PIN1 interaction, we verified that the ability for PIN1 to co-purify with GLI1 is significantly decreased in the presence of phosphatase (Figure 1*D*). We also note that GLI1 protein levels are increased in the presence of PIN1, which we propose is due to protein stabilization (see input controls in Figure 1*B* and Supplementary Figure 3*A*). Similarly, we analyzed GLI1 protein levels in the presence of an increasing level of either wild-type (WT) PIN1 or mutant PIN1^{W34A} in HEK293T cells. We observed that co-expression of WT PIN1, but not mutant PIN1^{W34A}, results in a greater GLI1 protein abundance (Figure 1*E*). These observations indicate that PIN1 leads to increased GLI1 protein abundance *in vitro*. Further investigation of the protein kinase responsible for the phosphorylation event leading to the regulation of the GLI1/PIN1 interaction as well as the molecular mechanisms involved in the PIN1-dependent regulation of GLI1 protein levels is warranted.

PIN1 Inhibition Impairs Hh Signaling

As a GLI1 interactor and regulator of GLI1 protein levels, PIN1 may contribute to the GLI1-mediated modulation of Hh target genes. To test this hypothesis, we investigated the effect of depletion of PIN1 on Hh signaling using an NIH3T3 Shh-Light2-based GLI-dependent luciferase reporter assay [35]. We observed that the Shh-N–mediated activation of Hh signaling is impaired in NIH3T3 Shh-Light2 cells upon the CRISPR/Cas9-mediated depletion of either GLI1 or PIN1 (Figure 2*A*). Next, we analyzed by quantitative reverse transcriptase (RT)-PCR the levels of expression of Hh target genes upon treatment with *SAG*, a chlorobenzothiophene-containing compound which acts as an SMO agonist, and *juglone,* a PIN1 inhibitor [36], in the MED-311FH cell line. In the presence of *SAG*, the levels of mRNA expression of *GLI1, PTCH1, PTCH2*, and *FOXA2* increase in MED-311FH (Figure 2*B*). Remarkably, we observed that the pharmacological inhibition of PIN1 by *juglone* in *SAG*-activated MED-311FH cells results in the strong reduction of the levels of expression of these Hh target genes (Figure 2*B*). Altogether, these results indicate that PIN1 is a positive regulator of Hh signaling.

Loss of Pin1 Suppresses Hh-Medulloblastoma Tumorigenesis In Vivo

In addition to the novel GLI1/PIN1 interaction, PIN1 has been previously shown to interact with other key modulators of Hh-medulloblastoma tumorigenesis [13,19–21]. We sought to investigate the loss of *Pin1 in vivo* using a genetically engineered mouse model of Hh-medulloblastoma tumorigenesis. *SmoA1* is an oncogenic gain-of-function allele of *Smo*[35], a key positive regulator of Hh signals [5,6]. The *ND2* or *GFAP* promoter-driven expression of *SmoA1* in mouse cerebellar granular neuron progenitor cells (CGNP), i.e., a "cell of origin" in Hh-medulloblastoma [37], results in CGNP hyperproliferation and medulloblastoma formation, as observed in the *ND2:SmoA1*[38] and the [*GFAP-tTA;TRE-SmoA1*] [28] mouse models of Hh-medulloblastoma. To assess *in vivo* the role of *Pin1* in medulloblastoma, we studied the genetic loss of *Pin1* in the bitransgenic [*GFAP-tTA;TRE-SmoA1*] model, where the expression of the tetracycline-regulated transactivators (*tTA*) is driven by a *GFAP* promoter and the expression of oncogenic *SmoA1* is under

the control of the tetracycline responsive element (*TRE*) [28]. Three groups of *C57BL/6* mice were studied: 1) a *TRE-SmoA1*–negative control group (*SmoA1* is not expressed in the absence of *GFAP-tTA*), 2) a positive control group of [*GFAP-tTA;TRE-SmoA1*] mice, which develops medulloblastoma; and 3) the [*GFAP-tTA;TRE-SmoA1;Pin1* $^{-/-}$] test group (genotyping data are available in Supplementary Figure 4). Each group was assessed by histological examination of the cerebellum by hematoxylin/eosin (H&E) staining, Ki67 (marker of proliferation) and NeuN (marker of neuronal differentiation) IHC, MRI evaluation, as well as Kaplan-Meier survival analysis.

At postnatal day (P)21, *TRE-SmoA1* mice exhibit normal cerebellar development with properly laminated molecular, Purkinje cell, and internal granular cell layers, as expected. Also expected at P21, the external granular cell layer has completely disappeared. Moreover, normal cerebellar neurons in the internal granular layer strongly stain for the neuronal marker NeuN and are in quiescent, nonproliferative stage, as demonstrated by the absence of staining for Ki-67 (Figure 3*A*). As previously described, [*GFAP-tTA;TRE-SmoA1*] mice develop medulloblastoma tumors detectable by histological analysis as early as P7, with 100% penetrance by P21 [28]. In P21 [*GFAP-tTA;TRE-SmoA1*] mice, large tumors can extend along the entire rostral-caudal length of the cerebellum; account for about a quarter of the total cerebellar volume; express NeuN, indicative of neuronal origin; and show marked proliferative activity (positive for Ki67) (Figure 3*A*). For comparison, two [*GFAP-tTA;TRE-SmoA1;Pin1* $^{-/-}$] mice were euthanized at P21 for histological analysis. The cerebellums of both [*GFAP-tTA;TRE-SmoA1;Pin1* $^{-/-}$] mice exhibit well-formed folia with normal lamination of the cerebellar cortex, and only minimal, microscopic evidence of early tumor development is observed (best appreciated by NeuN and Ki67 stainings in Figure 3*A*). The cerebellums of these two mice were entirely sectioned and analyzed; the microscopic tumors comprised <5% of the cerebellar volume.

CNS presentation was also assessed by MRI for a P56 [*GFAP-tTA;TRE-SmoA1;Pin1* $^{-/-}$] animal and its [*GFAP-tTA;TRE-SmoA1*] littermate. Whereas the pathophysiological effects can be appreciated in the [*GFAP-tTA;TRE-SmoA1*] mouse with the observation of dilated ventricles and subarachnoid spaces as well as significant doming of the skull, MRI analysis of the [*GFAP-tTA;TRE-SmoA1;Pin1* $^{-/-}$] mouse brain revealed no such signs of tumor burden (Figure 3*B*). *In vitro*, PIN1 promotes Hh signaling (Figure 2). We analyzed the level of mRNA expression of Hh target genes in the cerebellums of [*GFAP-tTA;TRE-Smoa1;Pin1* $^{-/-}$] mice and their [*GFAP-tTA;TRE-Smoa1*] littermates. As shown in Supplementary Figure 5, the level of expression of *Gli1, Gli2, Ptch2, Hhip1*, and *Foxa2* is significantly reduced in the cerebellums of [*GFAP-tTA;TRE-SmoA1;Pin1* $^{-/-}$] mice compared with the cerebellums of [*GFAP-tTA;TRE-SmoA1*] mice, in agreement with the *in vitro* data.

To assess the effect of loss of *Pin1* on normal cerebellar development, we also performed the histological analysis of P6 and P10 cerebellums isolated from *Pin1* KO mouse littermates. Cerebellums appear properly developed with normal foliation and normal lamination of the external granular cell, molecular, Purkinje cell, and internal granular cell layers. The external granular cell layer decreases in thickness as these cells begin to migrate through the molecular layer to produce the internal granular layer from P6 to P10, as expected (Supplementary Figure 6). Altogether, loss of *Pin1* has no noticeable histological effect on normal cerebellar development yet inhibits Hh-medulloblastoma tumorigenesis, thus echoing the genetic studies of loss of *Gli1* in physiological and pathophysiological contexts [30,31,34].

Finally, we performed a Kaplan-Meier survival analysis of the three aforementioned mouse groups. As previously described [28], [*GFAP-tTA;TRE-SmoA1*] animals succumb to medulloblastoma tumor within ~53 days. Remarkably, we observed that the median survival of the [*GFAP-tTA;TRE-SmoA1;Pin1* $^{-/-}$] mice is about three times greater than for [*GFAP-tTA;TRE-SmoA1*] mice (158 versus 53 days, respectively; $P = .0005$; Figure 3*C*). Although four of the seven [*GFAP-tTA;TRE-SmoA1;Pin1* $^{-/-}$] mice succumbed to medulloblastoma tumorigenesis at day 56, 75, 124, and 158, three of them survived beyond ~1 year. Moreover, the histological analysis of the cerebellums of two of these long-term survivors mice did not show evidence of tumor, either macroscopic or microscopic (>80% of each cerebellum was analyzed; Supplementary Figure 7). Thus, in agreement with our observations that PIN1 promotes GLI1 stability and Hh signaling, these *in vivo* analyses strongly support the hypothesis that *Pin1* plays an essential role in Hh-medulloblastoma tumorigenesis.

Discussion

We discovered a novel interaction between GLI1 and PIN1, and our *in vivo* analyses of *Pin1* in a genetically engineered *Smo*-induced mouse model of medulloblastoma tumorigenesis demonstrate that the loss of *Pin1* impairs tumor development and increases survival considerably. We speculate that the pro-oncogenic role of *Pin1* in Hh-medulloblastoma is not solely mediated via GLI1 but also via the regulation of other PIN1 targets [13,19–21]. Beyond its impact on disease progression, the potential of PIN1 as a therapeutic target in Hh-medulloblastoma is also dependent on the side effect associated with the inhibition of this protein during normal physiological development. Although *Pin1* KO mice display a range of cell-proliferative abnormalities, e.g., decreased body weight [13], they develop essentially normally [14]. The absence of any noticeable effect associated with the complete loss of *Pin1* on cerebellar development strongly suggests that therapeutic benefit may be achieved with tolerable doses of PIN1 inhibitors.

We are currently investigating whether pharmacological inhibition of PIN1 by either *juglone* or the flavonoid epigallocatechin gallate improves survival in mouse models of Hh-medulloblastoma. Interestingly, we note that quercetin, another flavonoid which inhibits PIN1, was recently identified in a chemical screen as a putative radiosensitizer for human medulloblastoma cells [39]. If our hypothesis is validated, i.e., PIN1 inhibitors can improve survival, it will strongly justify testing the clinical relevance of PIN1 blockade in Hh-medulloblastoma patients, either alone or in combination treatment regimens, e.g., in combination with SMO antagonists, which are currently being tested in clinical trials [40]. As a modulator of GLI1, the downstream position of *PIN1* in the Hh genetic pathway underscores its potential as a complement to SMO inhibition and may be specifically beneficial for overcoming resistance to SMO inhibitors [7], thereby paving the way toward a multitherapy approach to Hh-medulloblastoma. Beyond Hh-medulloblastoma, we speculate that *PIN1* can also modulate Hh signals in other neoplastic conditions in which Hh is involved [6]. Based on our findings, studies aiming to test the requirement of *Pin1* in mouse models of basal cell carcinoma [41], basaloid follicular hamartomas [42], and embryonal rhabdomyosarcoma [43] are highly justified and will help establish whether the role of *Pin1* in Hh-driven tumorigenesis is either general or specific to medulloblastoma.

Supplementary data to this article can be found online at http://dx.doi.org/10.1016/j.neo.2017.01.002.

Author Contributions

J. F. R. conceived and directed the project. T. X. and K. H. designed and performed the Y2H experiments. T. X., H. Z., S. S. P., and J. M. O. designed and performed the molecular and cellular studies. H. Z., L. E. M., C. U., T. U., A. D., S. C. P., and J. F. R. designed and performed the *in vivo* mouse studies. H. Z., S. C. P., S. V., and M. S. performed and analyzed the IHC experiments. H. Z., S. C. P., J. F. R., and A. S. performed and analyzed the MRI experiments. R. K. performed statistical analyses. J. F. R. wrote the manuscript, with contributions from other coauthors.

Acknowledgements

We thank UM Comprehensive Cancer Center Tissue for technical support with the IHC experiments, specifically Dafydd Thomas and Tina Fields; UM Vector Core Facility for the lentiviral sh-RNA plasmids; UM Center for Molecular Imaging for technical support with the MRI experiments, specifically Amanda Fair; CCSB for sharing ORFeome and Y2H clones. This work was supported by Padnos Fund for Innovative Cancer Research of the UM Comprehensive Cancer Center awarded to J. F. R.; Bench to Bedside Translation Award awarded to J. F. R. by the Michigan Institute for Clinical and Health Research and the National Center for Advancing Translational Sciences of the National Institutes of Health (NIH) under Award Number UL1TR000433; M-Cubed Grant awarded to J. F. R. and S. C. P.; grant R01CA155360 awarded to J. M. O. by the National Cancer Institute of the NIH; Seattle Children's Neuro-oncology endowment awarded to J. M. O; UM Cancer Center Support Grant (P30CA046592); and funds from the UM Department of Pathology provided to J. F. R. The sponsors were not involved in any of the following: study design; collection, analysis, and interpretation of data; the writing of the report; and the decision to submit the article for publication.

References

[1] Gajjar AJ and Robinson GW (2014). Medulloblastoma-translating discoveries from the bench to the bedside. *Nat Rev Clin Oncol* **11**, 714–722.

[2] Taylor MD, Northcott PA, Korshunov A, Remke M, Cho YJ, Clifford SC, Eberhart CG, Parsons DW, Rutkowski S, and Gajjar A, et al (2012). Molecular subgroups of medulloblastoma: the current consensus. *Acta Neuropathol* **123**, 465–472.

[3] Mulhern RK, Merchant TE, Gajjar A, Reddick WE, and Kun LE (2004). Late neurocognitive sequelae in survivors of brain tumours in childhood. *Lancet Oncol* **5**, 399–408.

[4] Laughton SJ, Merchant TE, Sklar CA, Kun LE, Fouladi M, Broniscer A, Morris EB, Sanders RP, Krasin MJ, and Shelso J, et al (2008). Endocrine outcomes for children with embryonal brain tumors after risk-adapted craniospinal and conformal primary-site irradiation and high-dose chemotherapy with stem-cell rescue on the SJMB-96 trial. *J Clin Oncol* **26**, 1112–1118.

[5] Ingham PW and AP McMahon (2001). Hedgehog signaling in animal development: paradigms and principles. *Genes Dev* **15**, 3059–3087.

[6] Amakye D, Jagani Z, and Dorsch M (2013). Unraveling the therapeutic potential of the Hedgehog pathway in cancer. *Nat Med* **19**, 1410–1422.

[7] Kool M, Jones DT, Jager N, Northcott PA, Pugh TJ, Hovestadt V, Piro RM, Esparza LA, Markant SL, and Remke M, et al (2014). Genome sequencing of SHH medulloblastoma predicts genotype-related response to smoothened inhibition. *Cancer Cell* **25**, 393–405.

[8] Lu KP, Hanes SD, and Hunter T (1996). A human peptidyl-prolyl isomerase essential for regulation of mitosis. *Nature* **380**, 544–547.

[9] Lu PJ, Zhou XZ, Shen M, and Lu KP (1999). Function of WW domains as phosphoserine- or phosphothreonine-binding modules. *Science* **283**, 1325–1328.

[10] Ranganathan R, Lu KP, Hunter T, and Noel JP (1997). Structural and functional analysis of the mitotic rotamase Pin1 suggests substrate recognition is phosphorylation dependent. *Cell* **89**, 875–886.

[11] Yaffe MB, Schutkowski M, Shen M, Zhou XZ, Stukenberg PT, Rahfeld JU, Xu J, Kuang J, Kirschner MW, and Fischer G, et al (1997). Sequence-specific and phosphorylation-dependent proline isomerization: a potential mitotic regulatory mechanism. *Science* **278**, 1957–1960.

[12] Liou YC, Zhou XZ, and Lu KP (2011). Prolyl isomerase Pin1 as a molecular switch to determine the fate of phosphoproteins. *Trends Biochem Sci* **36**, 501–514.

[13] Liou YC, Ryo A, Huang HK, Lu PJ, Bronson R, Fujimori F, Uchida T, Hunter T, and Lu KP (2002). Loss of Pin1 function in the mouse causes phenotypes resembling cyclin D1-null phenotypes. *Proc Natl Acad Sci U S A* **99**, 1335–1340.

[14] Fujimori F, Takahashi K, Uchida C, and Uchida T (1999). Mice lacking Pin1 develop normally, but are defective in entering cell cycle from G(0) arrest. *Biochem Biophys Res Commun* **265**, 658–663.

[15] Ryo A, Nakamura M, Wulf G, Liou YC, and Lu KP (2001). Pin1 regulates turnover and subcellular localization of beta-catenin by inhibiting its interaction with APC. *Nat Cell Biol* **3**, 793–801.

[16] Bao L, Kimzey A, Sauter G, Sowadski JM, Lu KP, and Wang DG (2004). Prevalent overexpression of prolyl isomerase Pin1 in human cancers. *Am J Pathol* **164**, 1727–1737.

[17] Wulf G, Garg P, Liou YC, Iglehart D, and Lu KP (2004). Modeling breast cancer in vivo and ex vivo reveals an essential role of Pin1 in tumorigenesis. *EMBO J* **23**, 3397–3407.

[18] Atkinson GP, Nozell SE, Harrison DK, Stonecypher MS, Chen D, and Benveniste EN (2009). The prolyl isomerase Pin1 regulates the NF-kappaB signaling pathway and interleukin-8 expression in glioblastoma. *Oncogene* **28**, 3735–3745.

[19] Moretto-Zita M, Jin H, Shen Z, Zhao T, Briggs SP, and Xu Y (2010). Phosphorylation stabilizes Nanog by promoting its interaction with Pin1. *Proc Natl Acad Sci U S A* **107**, 13312–13317.

[20] Rustighi A, Tiberi L, Soldano A, Napoli M, Nuciforo P, Rosato A, Kaplan F, Capobianco A, Pece S, and Di Fiore PP, et al (2009). The prolyl-isomerase Pin1 is a Notch1 target that enhances Notch1 activation in cancer. *Nat Cell Biol* **11**, 133–142.

[21] Shen M, Stukenberg PT, Kirschner MW, and Lu KP (1998). The essential mitotic peptidyl-prolyl isomerase Pin1 binds and regulates mitosis-specific phosphoproteins. *Genes Dev* **12**, 706–720.

[22] Yang X, Boehm JS, Salehi-Ashtiani K, Hao T, Shen Y, Lubonja R, Thomas SR, Alkan O, Bhimdi T, and Green TM, et al (2011). A public genome-scale lentiviral expression library of human ORFs. *Nat Methods* **8**, 659–661.

[23] Wang T, Wei JJ, Sabatini DM, and Lander ES (2014). Genetic screens in human cells using the CRISPR-Cas9 system. *Science* **343**, 80–84.

[24] Shalem O, Sanjana NE, Hartenian E, Shi X, Scott DA, Mikkelsen TS, Heckl D, Ebert BL, Root DE, and Doench JG, et al (2014). Genome-scale CRISPR-Cas9 knockout screening in human cells. *Science* **343**, 84–87.

[25] Liang L, Aiken C, McClelland R, Morrison LC, Tatari N, Remke M, Ramaswamy V, Issaivanan M, Ryken T, and Del Bigio MR, et al (2015). Characterization of novel biomarkers in selecting for subtype specific medulloblastoma phenotypes. *Oncotarget* **6**, 38881–38900.

[26] Longo PA, Kavran JM, Kim MS, and Leahy DJ (2013). Transient mammalian cell transfection with polyethylenimine (PEI). *Methods Enzymol* **529**, 227–240.

[27] Dreze M, Monachello D, Lurin C, Cusick ME, Hill DE, Vidal M, and Braun P (2010). High-quality binary interactome mapping. *Methods Enzymol* **470**, 281–315.

[28] Michael LE, Westerman BA, Ermilov AN, Wang A, Ferris J, Liu J, Blom M, Ellison DW, van Lohuizen M, and Dlugosz AA (2008). Bmi1 is required for Hedgehog pathway-driven medulloblastoma expansion. *Neoplasia* **10**, 1343–1349 [1345p following 1349].

[29] Lin W, Kemper A, McCarthy KD, Pytel P, Wang JP, Campbell IL, Utset MF, and Popko B (2004). Interferon-gamma induced medulloblastoma in the developing cerebellum. *J Neurosci* **24**, 10074–10083.

[30] Park HL, Bai C, Platt KA, Matise MP, Beeghly A, Hui CC, Nakashima M, and Joyner AL (2000). Mouse Gli1 mutants are viable but have defects in SHH signaling in combination with a Gli2 mutation. *Development* **127**, 1593–1605.

[31] Bai CB, Auerbach W, Lee JS, Stephen D, and Joyner AL (2002). Gli2, but not Gli1, is required for initial Shh signaling and ectopic activation of the Shh pathway. *Development* **129**, 4753–4761.

[32] Lauth M, Bergstrom A, Shimokawa T, and Toftgard R (2007). Inhibition of GLI-mediated transcription and tumor cell growth by small-molecule antagonists. *Proc Natl Acad Sci U S A* **104**, 8455–8460.

[33] Infante P, Mori M, Alfonsi R, Ghirga F, Aiello F, Toscano S, Ingallina C, Siler M, Cucchi D, and Po A, et al (2015). Gli1/DNA interaction is a druggable target for Hedgehog-dependent tumors. *EMBO J* **34**, 200–217.

[34] Kimura H, Stephen D, Joyner A, and Curran T (2005). Gli1 is important for medulloblastoma formation in Ptc1+/- mice. *Oncogene* **24**, 4026–4036.

[35] Taipale J, Chen JK, Cooper MK, Wang B, Mann RK, Milenkovic L, Scott MP, and Beachy PA (2000). Effects of oncogenic mutations in Smoothened and Patched can be reversed by cyclopamine. *Nature* **406**, 1005–1009.

[36] Hennig L, Christner C, Kipping M, Schelbert B, Rucknagel KP, Grabley S, Kullertz G, and Fischer G (1998). Selective inactivation of parvulin-like peptidyl-prolyl cis/trans isomerases by juglone. *Biochemistry* **37**, 5953–5960.

[37] Yang ZJ, Ellis T, Markant SL, Read TA, Kessler JD, Bourboulas M, Schuller U, Machold R, Fishell G, and Rowitch DH, et al (2008). Medulloblastoma can be initiated by deletion of Patched in lineage-restricted progenitors or stem cells. *Cancer Cell* **14**, 135–145.

[38] Hallahan AR, Pritchard JI, Hansen S, Benson M, Stoeck J, Hatton BA, Russell TL, Ellenbogen RG, Bernstein ID, and Beachy PA, et al (2004). The SmoA1 mouse model reveals that notch signaling is critical for the growth and survival of sonic hedgehog-induced medulloblastomas. *Cancer Res* **64**, 7794–7800.

[39] Lagerweij T, Hiddingh L, Biesmans D, Crommentuijn MH, Cloos J, Li XN, Kogiso M, Tannous BA, Vandertop WP, and Noske DP, et al (2016). A chemical screen for medulloblastoma identifies quercetin as a putative radiosensitizer. *Oncotarget* **7**, 35776–35788.

[40] Robinson GW, Orr BA, Wu G, Gururangan S, Lin T, Qaddoumi I, Packer RJ, Goldman S, Prados MD, and Desjardins A, et al (2015). Vismodegib Exerts Targeted Efficacy Against Recurrent Sonic Hedgehog-Subgroup Medulloblastoma: Results From Phase II Pediatric Brain Tumor Consortium Studies PBTC-025B and PBTC-032. *J Clin Oncol* **33**, 2646–2654.

[41] Grachtchouk M, Mo R, Yu S, Zhang X, Sasaki H, Hui CC, and Dlugosz AA (2000). Basal cell carcinomas in mice overexpressing Gli2 in skin. *Nat Genet* **24**, 216–217.

[42] Grachtchouk V, Grachtchouk M, Lowe L, Johnson T, Wei L, Wang A, de Sauvage F, and Dlugosz AA (2003). The magnitude of hedgehog signaling activity defines skin tumor phenotype. *EMBO J* **22**, 2741–2751.

[43] Hatley ME, Tang W, Garcia MR, Finkelstein D, Millay DP, Liu N, Graff J, Galindo RL, and Olson EN (2012). A mouse model of rhabdomyosarcoma originating from the adipocyte lineage. *Cancer Cell* **22**, 536–546.